

Connecting host physiology to host resistance in the conifer-bark beetle system

William A. Nelson · Mark A. Lewis

Received: 12 May 2007 / Accepted: 20 February 2008
© Springer Science + Business Media B.V. 2008

Abstract Host defenses can generate Allee effects in pathogen populations when the ability of the pathogen to overwhelm the defense system is density-dependent. The host–pathogen interaction between conifer hosts and bark beetles is a good example of such a system. If the density of attacking beetles on a host tree is lower than a critical threshold, the host repels the attack and kills the beetles. If attack densities are above the threshold, then beetles kill the host tree and successfully reproduce. While the threshold has been found to correlate strongly with host growth, an explicit link between host physiology and host defense has not been established. In this article, we revisit published models for conifer-bark beetle interactions and demonstrate that the stability of the steady states is not consistent with empirical observations. Based on these results, we develop a new model that explicitly describes host damage caused by the pathogen and use the physiological characteristics of the host to relate host growth to defense. We parameterize the model for

mountain pine beetles and compare model predictions with independent data on the threshold for successful attack. The agreement between model prediction and the observed threshold suggests the new model is an effective description of the host–pathogen interaction. As a result of the link between the host–pathogen interaction and the emergent Allee effect, our model can be used to better understand how the characteristics of different bark beetle and host species influence host–pathogen dynamics in this system.

Keywords Host–pathogen models · Attack threshold · Allee effect · Bark beetles · Resin defenses · Mountain pine beetles · Carbon budget model

Introduction

Hosts can generate Allee effects (Allee 1931) in a pathogen population when host defense depends on pathogen densities (Courchamp et al. 1999; Ogden et al. 2002; Uma Devi and Uma Maheswara Rao 2006). Bark beetles are a classic example of a pathogen that suffers an Allee effect from host resistance (Berryman 1979). Bark beetles are a common and destructive pathogen of pine forests (Logan and Powell 2001) that must kill host tissue to ensure successful survival and reproduction (Christiansen et al. 1987; Raffa et al. 2005). As a result of host defenses, many individual beetles are required to successfully overwhelm and kill a single host tree (e.g., Christiansen et al. 1987; Fig. 1). Most species of bark beetles have evolved a pheromone communication system that helps aggregate the beetle population during flight (Raffa 2001). If insufficient beetles are available to attack a host, then host defenses kill

W. A. Nelson (✉)
Department of Biological Sciences, University of Alberta,
Edmonton, Alberta, Canada
e-mail: nelsonw@queensu.ca

M. A. Lewis
Department of Mathematical and Statistical Sciences,
University of Alberta, Edmonton, Alberta, Canada
e-mail: mlewis@math.ualberta.ca

Present Address:
W. A. Nelson
Department of Biology, Queen's University,
Kingston, Ontario, Canada

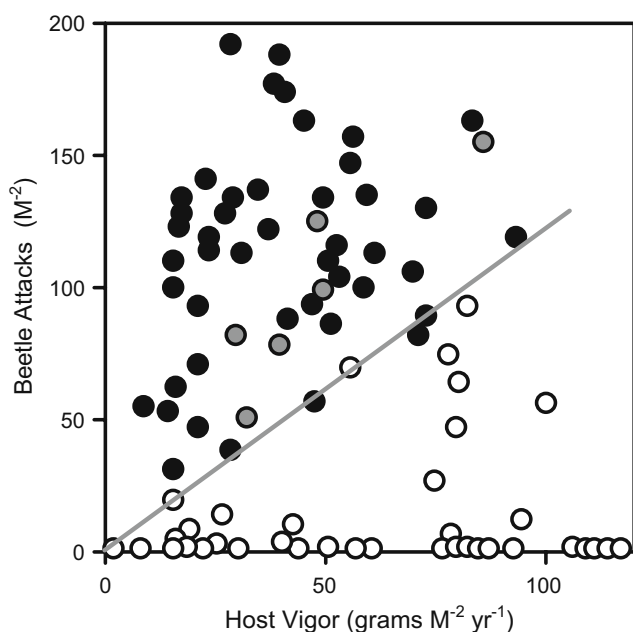


Fig. 1 Empirical threshold for successful attack of mountain pine beetles as a function of host vigor (data from Waring and Pitman 1985). Vigor is defined as the mass of wood added to a host tree per year divided by the leaf area. Each *symbol* represents an individual tree. *Solid circles* indicate trees killed by beetles, *open circles* are living trees that resisted beetle attack, and *gray circles* are living trees where a portion of the bark area was killed by beetles. The *gray line* is the empirically estimated threshold for host mortality

the attacking beetles. If the attack density is above a critical threshold, then attacking beetles kill the host tree and successfully reproduce. Because beetle survival is tightly coupled to host defense, the threshold for successful attack on an individual tree produces a population-level Allee effect in bark beetles (Berryman and Stenseth 1989). Owing to the close host–pathogen interaction between conifer trees and bark beetles, as well as the economic impact of this pest species, a good deal of empirical and theoretical research has been carried out.

A number of models have been developed to describe the host–pathogen interaction in bark beetles (Berryman et al. 1989; Stenseth 1989; Powell et al. 1996). However, these models blend two distinct processes: the host–pathogen interaction within the tree and the immigration of new beetles to the host tree. Biologically, these processes can be separated because they occur over different time scales. Beetle immigration is mediated by aggregation pheromones that are generated by beetles in the process of attacking a host tree. These pheromones can attract additional beetles to the host tree from those flying in the local vicinity (Raffa 2001). Such pheromone-mediated immigration

occurs at the start of an attack and lasts less than a week (e.g., Raffa and Berryman 1983). In contrast, host death from high attack densities occurs between 4 and 6 weeks after the attack has started (Kirisits and Offenthaler 2002). The difference in time scales suggests that the host–pathogen interaction operates at a slower rate than beetle migration. This is also supported by empirical observations of the attack threshold (e.g., Fig. 1), that are well described by the beetle attack density after all migration has occurred. Thus, from the perspective of the host–pathogen interaction, the effect of pheromone-mediated immigration can be thought of as influencing initial attack density.

In this article, we analyze existing bark beetle models in the absence of recruitment from flying beetles to study the core host–pathogen interaction. Our results reveal that these modified models predict unrealistic steady state characteristics, suggesting that current descriptions of the beetle–host interaction need further development. Based on these results, we develop a new model of the beetle–host interaction that explicitly describes host damage and demonstrate that it has biologically realistic steady state characteristics. Using what is known about tree physiology, we then derive a link between host growth and resin production under the assumption that growth in carbohydrate is limited. In doing so, we provide the first model to integrate physiologically based host resin defense with process-based attacking beetle dynamics. We parameterize the model for mountain pine beetles using literature data and compare model predictions against independent empirical data on the attack threshold in mountain pine beetles. The success of our new model at predicting the empirical threshold suggests the new model reflects a more accurate description of the beetle–host interaction that can be used to understand how the characteristics of the host–pathogen interaction influence beetle population dynamics.

Reanalysis of published models

To begin, we reanalyze previous models of the host–pathogen interaction in the absence of recruitment from flying beetles.

Berryman et al. (1989) and Stenseth (1989)

One of the earlier models of the host–pathogen interaction was developed by Berryman et al. (1989). A similar model is presented in Stenseth (1989), which is analyzed in Appendix A. Berryman et al. (1989)

developed a model of the beetle–host interaction that explicitly describes the processes of beetle attack, host resin defense, and immigration from flying beetles. The model is given by

$$\frac{dA}{dt} = \overbrace{b_1(b_2 - b_3 R)AR}^{\text{beetle recruitment}} - \overbrace{b_4 AR}^{\text{mortality}} \tag{1}$$

$$\frac{dR}{dt} = \overbrace{b_5(1 - b_6 A)}^{\text{resin production}} - \overbrace{b_7 R}^{\text{resin loss}} \tag{2}$$

where $A(t)$ is the density of attacking beetles per tree and $R(t)$ is the volume of resin per beetle gallery. The first term of Eq. 1 is recruitment from flying beetles due to host attractiveness, where b_1 is the size of the local flying beetle population and parameters b_2 and b_3 reflect the attractiveness/repellency of the as a function of resin volume. The second term is beetle mortality, where b_4 is the rate at which per capita mortality increases with resin volume. Equation 2 describes resin dynamics in the host, where b_5 is the maximum rate of resin production of the host, b_6 is the decrease in resin production caused by attacking beetles, and b_7 is the resin loss rate through the attack holes.

Because we are interested in studying beetle–host dynamics in the absence of immigration from flying beetles, we remove the recruitment term from Eq. 1. Introducing the following dimensionless variables

$$\tilde{A} = Ab_6, \tilde{R} = R \frac{b_7}{b_5}, \tilde{t} = tb_7$$

and the dimensionless parameter

$$\alpha = \frac{b_4 b_5}{b_7^2}$$

we can write a dimensionless version of the modified model as (after dropping the tildes)

$$\frac{dA}{dt} = -\alpha AR \tag{3}$$

$$\frac{dR}{dt} = 1 - A - R \tag{4}$$

The model given by Eqs. 3 and 4 has two steady states. The first is $(A^*, R^*) = (0, 1)$, which is a steady state where the tree is alive and all attacking beetles are dead. The second is $(A^*, R^*) = (1, 0)$, which is a steady

state where the beetles have successfully killed the host tree. The Jacobian of Eqs. 3 and 4 is given by

$$\mathbf{J}_{(A^*, R^*)} = \begin{pmatrix} -\alpha R^* & -\alpha A^* \\ -1 & -1 \end{pmatrix} \tag{5}$$

At the steady state $(A^*, R^*) = (0, 1)$, both eigenvalues are negative, which means that the tree-alive steady state is stable. At the steady state $(A^*, R^*) = (1, 0)$, one eigenvalue is negative and one is positive. Thus, the tree-dead steady state is an unstable saddle. An unstable tree-dead steady state means that beetles do not kill host trees in the absence of continual recruitment from flying beetles, regardless of the initial density of attacking beetles. However, because continual beetle immigration is not a requirement for host death in nature, one or more of the key biological interactions is missing from the model of Berryman et al. (1989). Figure 2 shows the isoclines, steady states, and example phase plane trajectories.

Powell et al. (1996)

Powell et al. (1996) developed a mechanistic model of beetle dispersal and attack that describes the dynamics of flying beetles, attacking beetles, host resin, and pheromones. The model is spatially explicit, and it is described by a set of six partial differential equations. To extract the beetle–host interaction in the absence of

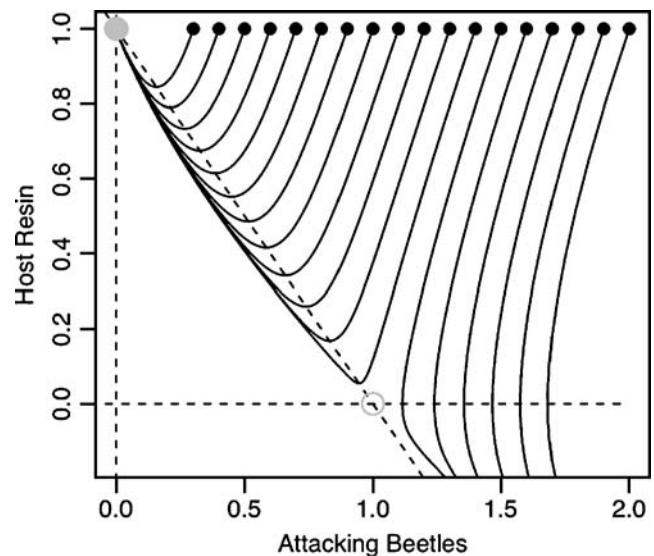


Fig. 2 Example trajectories for the model of Berryman et al. (1989) in the absence of recruitment from flying beetles. Dashed lines show the attacking beetle and resin isoclines. Gray circles depict the steady states; the solid circle is a stable steady state and the open circle is unstable. The black lines are example trajectories for $\alpha = 0.5$, and solid black circles denote initial conditions

flying beetle recruitment, we assume that the density of attacking beetles changes only as a result of mortality from host defenses. With this assumption, the beetle–host interaction is described by the following set of equations

$$\frac{dA}{dt} = -p_1 AR \quad (6)$$

$$\frac{dH}{dt} = -p_5 HR \quad (7)$$

$$\frac{dR}{dt} = p_2(p_3 - R)R - p_4 HR \quad (8)$$

where $A(t)$ is the density of beetles attacking a host, $H(t)$ is the number of holes in a host produced by the attacking beetles, and $R(t)$ is the abundance of resin in a host. From Eq. 6, the attacking beetle density declines from resin-caused mortality, where p_1 is the rate at which the per capita beetle mortality rate increases with resin. Resin is lost through the holes bored by attacking beetles, where p_5 is the rate at which the hole-filling rate increases with resin abundance. If we assume that each attacking beetle bores a single hole, then $H(0) = H_o = A_o$. Resin production is described by the first term of Eq. 8, where p_2 is the maximum per capita rate of resin renewal and p_3 is the maximum amount of resin in the absence of attacking beetles. Powell et al. (1996) consider that host vigor is described by p_3 ; the maximum capacity of the host to hold resin. However, as we show below, p_3 drops out in the process of nondimensionalization. As an alternative, we consider p_2 a measure of host vigor because it reflects the ability of the host to produce resin and does not drop out in the process of nondimensionalization.

Because the resin dynamics given by Eq. 8 are independent of attacking beetle density, the model dynamics can be understood by studying the coupled Eqs. 7 and 8. We introduce the following dimensionless variables

$$\tilde{H} = \frac{H}{p_3} \frac{p_4}{p_5}, \quad \tilde{R} = R \frac{1}{p_3}, \quad \tilde{t} = tp_3 p_5$$

and dimensionless parameter

$$\beta = \frac{p_2}{p_5}$$

to write the modified dimensionless model as (after dropping the tildes)

$$\frac{dH}{dt} = -HR \quad (9)$$

$$\frac{dR}{dt} = \beta(1 - R)R - HR \quad (10)$$

The model given by Eqs. 9–10 has two steady states. The first is $(H^*, R^*) = (0, 1)$, which is a steady state where the tree is alive and the attacking beetles are dead. The second steady state is $(H^*, R^*) = (\tilde{H}, 0)$, where \tilde{H} can be any value between zero and the initial number of holes (i.e., $0 \leq \tilde{H} \leq H_o$). More precisely, \tilde{H} is an infinite set of steady states that all satisfy Eqs. 9 and 10 at equilibrium (Fig. 3). Biologically, the infinite set of steady states reflects a situation where the host has been killed and a variable number of holes and attacking beetles remain alive. The number of holes remaining depends on the outcome of the dynamical process and, thus, on the initial number attacking beetles and the parameter β . For brevity, we refer to the infinite set of steady states simply as a *steady state* in the text below. The stability analysis is presented in Appendix B. Similar to the modified Berryman et al. (1989) model, the tree-alive steady state given by $(H^*, R^*) = (0, 1)$ is stable. The tree-dead steady state is also stable if $\tilde{H} > \beta$, but it is unstable if $\tilde{H} < \beta$. As a result, the host–pathogen interaction at the core of the Powell et al. (1996) model does not have the characteristics observed in nature. Figure 3 shows the isoclines, steady states, and example phase plane trajectories for the model given by Eqs. 10 and 9.

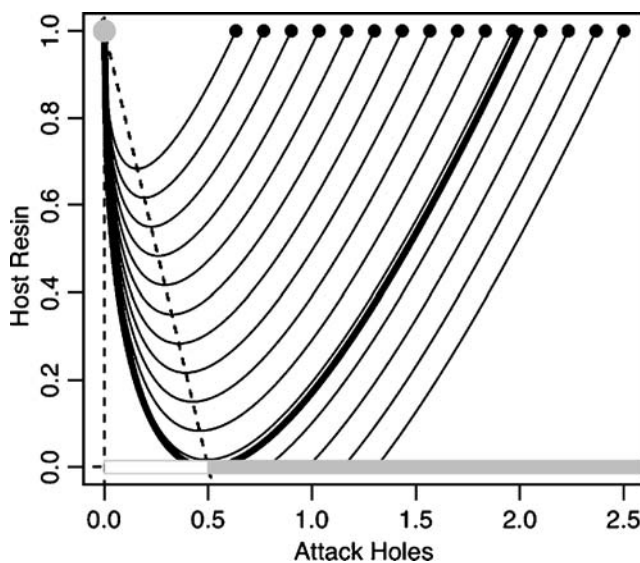


Fig. 3 Phase plane diagram for the beetle–host model of Powell et al. (1996) in the absence of recruitment from flying beetles. *Dashed lines* show the attacking hole and resin isoclines. The *gray symbols* are steady states; the *circle* represents a point steady state and the *thick line* represents an infinite set of steady states. *Solid symbols* are stable steady states and *open symbols* are unstable. The transition between unstable and stable regions of the dead host steady state (*thick gray line*) occurs when $\tilde{H} = \beta$. The *black lines* show example trajectories for $\beta = 0.5$, and the separatrix is shown in *bold*

A new model for the host–pathogen interaction

Empirical data on the threshold for bark beetle survival (e.g., Mulock and Christiansen 1986; Fig. 1) suggest that the process of aggregation, whereby flying beetles are attracted to new hosts by the pheromones emitted from attacking beetles, does not have a direct influence on the beetle–host interaction beyond determining the initial attack density. Our reanalysis of the published models by Berryman et al. (1989), Stenseth (1989), and Powell et al. (1996) reveals that, when flying beetle recruitment is removed from the beetle–host interaction, the dead-host steady state becomes unstable for some parameter values. Biologically, this implies that trees cannot be killed without continuous beetle immigration, which is not what occurs in nature. In the next section, we develop a new model of the beetle–host interaction that resolves this problem by explicitly including host damage caused by attacking beetles. As above, we assume that the process of beetle aggregation can be subsumed into the initial attack density (see Appendix E for validation of this assumption). We begin by developing a general model that describes the beetle–host interaction with undefined functions and study the steady states. In the next section, we consider a linear form of the general model and study the characteristics and stability of the emergent threshold for bark beetle survival.

General model

Resin production by a host tree is considered the primary mechanism of defense against bark beetles (Christiansen et al. 1987; Franceschi et al. 2005). Prior to an attack, the phloem tissue contains some amounts of preformed resin, which is referred to as the constitutive defense. At the start of an attack, resin is produced in the phloem tissue around the attack site (referred to as the induced defense) (Christiansen et al. 1987; Lewinsohn et al. 1991; Raffa and Smalley 1995). Induced resin is derived from carbohydrates in the phloem tissue surrounding the attack site (Trapp and Croteau 2001). Because carbohydrates are produced by photosynthesis in the leaves, both the production and the transport of carbohydrates to the attack site become determinants of resin production (Christiansen et al. 1987). This process of induced defense is well supported by empirical evidence, which demonstrates that interfering with the host’s ability to supply or transport carbohydrates has a large influence on resin production and the ability of the host to defend against bark beetle attack (Lombardero et al. 2000; Wallin and Raffa 2001;

Miller and Berryman 1986). Phloem tissue is composed of densely packed sieve tubes and is the main transport path for carbohydrates from the leaves to the attack sites. As a result, attacking beetles can interfere with host defense by either diluting resin production among numerous attack sites or by damaging phloem tissue and thereby reducing carbohydrate transport.

These empirical observations suggest that a dynamic model of both constitutive and induced defenses requires three components: resin volume, attacking beetles, and the undamaged phloem tissue necessary for carbohydrate transport. Similar to the previously published models, the model proposed here includes the ability of the host to produce resin. The key modification is an explicit representation of damage to the carbohydrate transport pathway. In general, such a model can be described by

$$\frac{dA}{dt} = -Ah(R) \quad (11)$$

$$\frac{dS}{dt} = -Sk(A) \quad (12)$$

$$\frac{dR}{dt} = Sf(R) - Rg(A) \quad (13)$$

where $A(t)$ is the number of attacking beetles still alive in the tree, $S(t)$ is the number of undamaged sieve tubes in the tree, and $R(t)$ is the resin volume of the host tree. The function $f(R)$ describes the rate of resin production per undamaged sieve tube. As such, it is a phenomenological representation of carbohydrate production, carbohydrate transport, and conversion of carbohydrates to resin.

Carbohydrate transport through sieve tubes is governed by osmoregulatory flow (Thompson and Holbrook 2003), which suggest that resin production should be at a maximum f_m when no resin is present (i.e., $f(0) = f_m$) and decrease with increasing resin volume (i.e., $f'(R) < 0$) until it reaches zero at the maximum resin capacity R_m (i.e., $f(R_m) = 0$). The function $g(A)$ describes resin metabolism by beetles, which we assume is a monotonically increasing function of beetle density (i.e., $g'(A) > 0$) that goes to zero when there are no attacking beetles still alive (i.e., $g(0) = 0$). Attacking beetle dynamics are given by Eq. 11, where the function $h(R)$ describes beetle mortality due to resin. Empirical data suggest that greater amounts of resin cause greater mortality rates in beetles (e.g., Raffa and Smalley 1995), so we constrain the function $h(R)$ to be a monotonically increasing function of resin abundance (i.e., $h'(R) > 0$)

with the constraint that $h(0) = 0$. We model the sieve tube damage caused by attacking beetles (including any associated fungus) as a per capita sieve tube loss rate $k(A)$ that increases monotonically with the number of attacking beetles still alive (i.e., $k'(A) > 0$), and with the constraint that $k(0) = 0$. The host is dead when all the sieve tubes are damaged (i.e., $S = 0$). The definitions and constraints for the general model are summarized in Table 1.

Steady state solutions

The constraints described above are sufficient to determine steady states of the general model, without the need to specify functions. The model given by Eqs. 11–13 has three steady states: $(A^*, S^*, R^*) = (\bar{A}, 0, 0)$, $(0, 0, \bar{R})$, and $(0, \bar{S}, R_m)$. \bar{A} is the final number of attacking beetles and can be any value between zero and the initial number of attacks (i.e., $0 \leq \bar{A} \leq A_o$). Similarly, \bar{R} is the final resin volume between zero and the initial resin volume (i.e., $0 \leq \bar{R} \leq R_o$), and \bar{S} is the final number of sieve tubes between zero and the initial number (i.e., $0 \leq \bar{S} \leq S_o$).

Biologically, the steady states are qualitatively similar to those predicted by the previously published models. At the steady state $(A^*, S^*, R^*) = (0, \bar{S}, R_m)$, all attacking beetles are dead and the host tree is at maximum resin capacity with some amount of undamaged sieve tubes remaining. The proportion of damaged sieve tubes indicates the amount of permanent damage caused by the unsuccessful beetle attacks (i.e., $1 - \bar{S}/S_o$). At the steady state $(A^*, S^*, R^*) = (\bar{A}, 0, 0)$, the attacking beetles have damaged all sieve tubes and killed the host tree. The last steady state is given by $(A^*, S^*, R^*) = (0, 0, \bar{R})$, which reflects a situation where the attacking beetles damaged all of the host sieve tubes and the remaining resin was sufficient to kill the beetles, with the end result that both the beetles and host are dead.

Linear model

We consider a model with linear functions. Let $f(R) = f_o \left(1 - \frac{R}{R_m}\right)$, $g(A) = g_o A$, $h(R) = h_o R$, and $k(A) = k_o A$. Parameter f_o is the maximum resin production rate per sieve tube, R_m is the maximum resin volume, g_o is the rate at which the resin loss rate changes with the number of attacking beetles, h_o is the rate at which beetle mortality changes with resin volume, and k_o is the rate at which the sieve tube loss rate changes with the number of attacking beetles. Introducing the following dimensionless variables

$$\tilde{A} = \frac{A g_o}{h_o R_m}, \tilde{S} = \frac{S}{S_o}, \tilde{R} = \frac{R}{R_m}, \tilde{t} = t h_o R_m \tag{14}$$

and dimensionless parameters

$$\gamma = \frac{S_o f_o}{R_m^2 h_o}, \zeta = \frac{k_o}{g_o} \tag{15}$$

allows us to write the following dimensionless model (after dropping the tildes)

$$\frac{dA}{dt} = -AR \tag{16}$$

$$\frac{dS}{dt} = -\zeta AS \tag{17}$$

$$\frac{dR}{dt} = \gamma S(1 - R) - AR \tag{18}$$

The nondimensional steady states are $(\bar{A}, 0, 0)$, $(0, 0, \bar{R})$, and $(0, \bar{S}, 1)$, where $0 \leq \bar{A} < \infty$, $0 \leq \bar{R} \leq 1$, and $0 \leq \bar{S} \leq 1$. The initial conditions are $(A_o, 1, R_o)$, where $0 \leq R_o \leq 1$ and $0 \leq A_o \leq \infty$. The two steady states of biological interest are the live beetle – dead host state $(A^*, S^*, R^*) = (\bar{A}, 0, 0)$ – and the dead beetle—live host state $(A^*, S^*, R^*) = (0, \bar{S}, 1)$. Both of these steady states are stable for γ and \bar{A} slightly greater than zero (Appendix C). Thus, and in contrast to our reanalysis of published models, the host–

Table 1 Symbol definitions and constraints for the general model

Symbol	Definition	Constraints
A	Number of attacking beetles per tree	$A \geq 0$
S	Number of sieve tubes per tree	$S \geq 0$
R	Resin volume per tree	$R \geq 0$
t	Time index	–
R_m	Maximum resin volume per tree	$R_m \geq 0$
f_m	Maximum resin production rate	$f_m \geq 0$
$f(R)$	Per capita resin production function	$f(0) = f_m, f(R_m) = 0, f'(R) < 0$
$g(A)$	Per capita resin loss rate	$g(0) = 0, g'(A) > 0$
$h(R)$	Per capita beetle mortality function	$h(0) = 0, h'(R) > 0$
$k(A)$	Per capita sieve tube damage rate	$k(0) = 0, k'(A) > 0$

pathogen model developed here has steady states that are consistent with empirical observations.

Dynamics of the linear model given by Eqs. 16–18 are governed by two parameters γ and ζ . Biologically, γ is the ratio of maximum resin production to maximum beetle mortality and ζ is the ratio of the phloem damage rate to the resin removal rate. To understand the magnitude of initial attack density required to kill a host tree, and how this is influenced by the parameters, we study the threshold behavior using numerical simulations of the model trajectories. Figure 4 shows example trajectories of the linear model. At high initial

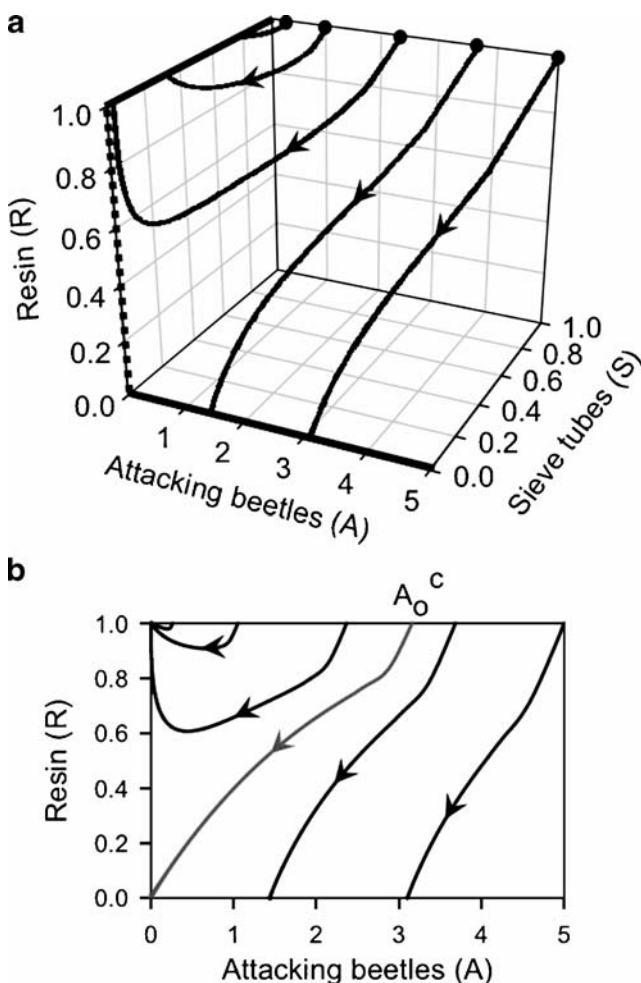


Fig. 4 Example trajectories for the linear model given by Eqs. 16–18. Each line shows a trajectory starting from different initial beetle densities A_o . The dynamics are shown for $\gamma = 8$ and $\zeta = 1$, and arrows show the direction of time. **a** Trajectories in the full 3D phase space. Circles are initial conditions, and the bold lines are steady states. Solid lines are stable steady states, and the dashed line is the unstable steady state. **b** Projection of the 3D trajectories onto the R - A plane. The gray line shows the trajectory emerging from the critical initial beetle abundance A_o^c , above which beetle attacks kill the host tree and below which the host kills the attacking beetles

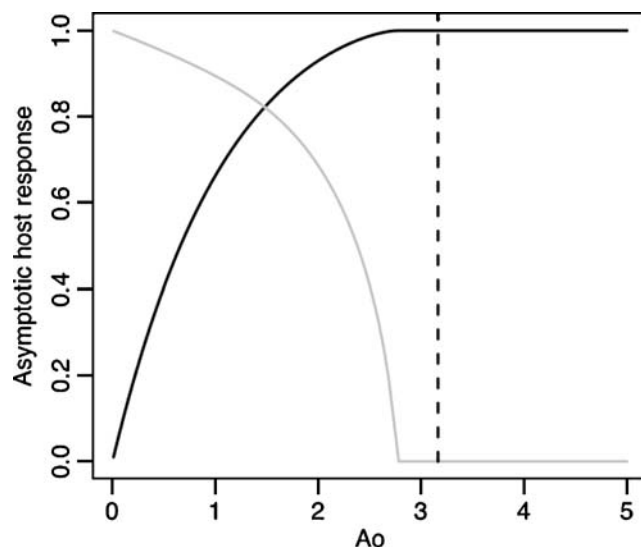


Fig. 5 Asymptotic host responses. Proportion of host damaged after the attack process ($(1 - S^*)$; black line) and the minimum resin abundance (gray line) for parameter values shown in Fig. 4. The critical attack density (A_o^c) is shown with the dashed line

beetle abundance, beetles quickly kill the host tree. As the number of initial beetles decreases, the host is still killed but the number of beetles remaining also decreases. Below the critical initial beetle abundance A_o^c , the host repels the attack and all beetles are killed. Further decreases in the initial beetle abundance have the effect of reducing the level of damage sustained by the host before the beetles are killed. The critical initial beetle abundance A_o^c is defined as the value of A_o that results in $(A^*, S^*, R^*) = (0, 0, 0)$ and represents the threshold for beetle survival. Because there is no analytical solution to Eqs. 16–18, we determined A_o^c numerically. When host trees survive attacks, the resulting damage and resin densities depend on the initial density of attacking beetles (Fig. 5). Even if attack densities are lower than the critical threshold, the host tree can still suffer substantial damage.

The critical threshold A_o^c depends on parameters γ and ζ . The empirical observations of Fig. 1 indicate that greater numbers of beetles are required to kill hosts with higher levels of vigor. For these data, vigor is defined as the volume of wood produced per year relative to the leaf area, which reflects growth efficiency of the host (Waring et al. 1980). The rationale for studying the influence of host vigor on the threshold for successful beetle attack is that trees able to produce greater amounts of wood have higher carbohydrate production and, thus, should also be able to produce greater amounts of resin if attacked. We develop this link quantitatively in the next section. Qualitatively, however, greater host vigor corresponds to greater resin

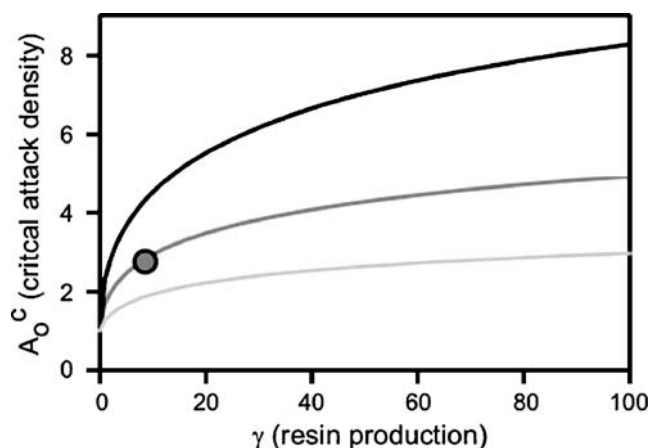


Fig. 6 Critical threshold of initial attacking beetle abundance A_o^c as a function of host resin production for the linear model given by Eqs. 16–18. Thresholds are shown for $\zeta = 0.5$ (black line), $\zeta = 1$ (dark gray line), and $\zeta = 2$ (light gray line). The gray point shows the critical attack density (A_o^c) for the gray trajectory of Fig. 4

production. In the linear model, this is the γ parameter. Figure 6 shows how the critical threshold changes as a function of γ .

The linear model predicts that the threshold A_o^c should increase with increasing ability of the host to produce resin. Qualitatively, this agrees well with the empirical data (Fig. 1). In the following section, we link resin production to host vigor quantitatively and fully parameterize the model for mountain pine beetles using independent literature data. To assess the relevance of the mechanisms described by the model, we then compare the quantitative predictions from the linear model with the empirical threshold of Fig. 1.

Parameterization of the linear model

Linking host vigor to resin production

Carbohydrate production for a tree can be described by $l_o L$, where L is the leaf area of the tree and l_o is the per-unit leaf area rate of carbohydrate production that includes the cumulative influence of environmental factors such as light levels and temperature (e.g., Zhang et al. 1994). Carbohydrates produced by the tree will eventually get used for respiration, growth, and resin defense. Tree respiration is partitioned into two components: maintenance respiration and growth respiration (e.g., Vanninen and Mäkelä 2005). Maintenance respiration is proportional to tree mass W , and growth respiration is proportional to carbohydrate production.

Thus, the net amount of carbon available Ψ for growth and defence can be described by

$$\Psi = \mu L - \sigma W \quad (19)$$

where μ is the per-unit leaf area rate of carbohydrate production prior to discounting growth respiration, and σ is the per-unit mass maintenance costs.

Much research suggests that the net photosynthate is preferentially allocated to growth prior to damage (e.g., Lombardero et al. 2000; Turtola et al. 2003). If we assume that growth is limited by the availability of carbohydrates (rather than nutrients), that μ and σ are average yearly rates, and that L and W can be considered constant during the year (growth incremented between years), then the amount of wood mass added to a tree G_w in a given year is given by

$$G_w = \Psi(1 - m_w)c_w \quad (20)$$

where m_w is the per capita cost of producing wood and c_w is the conversion from carbon mass into wood mass. Host vigor ν is often measured as the amount of mass added to a tree each year, divided by the leaf area (Waring et al. 1980). From Eq. 20, this can be expressed as

$$\nu = \frac{G_w}{L} = \frac{\Psi(1 - m_w)c_w}{L} \quad (21)$$

Once beetles begin attacking a host, we assume that all available carbohydrates are directed to resin production as required, which is known as the *growth-differentiation* hypothesis (Loomis 1932). This means that the maximum rate of resin production is governed by the maximum carbohydrate production. The total amount of resin produced per year G_r is then given by

$$G_r = \Psi(1 - m_r)c_r \quad (22)$$

where m_r is the per capita cost of producing resin and c_r is the conversion from carbon mass into resin mass. In the linear model, the maximum rate of resin production is given by $f_o S_o$, where f_o is the per-sieve rate of resin production when resin abundance is zero and S_o is the initial number of sieve tubes. Thus, the maximum rate of resin production in the linear model $f_o S_o$ can be related to net carbohydrate production by

$$f_o S_o = \frac{G_r t_r}{\delta_r} \quad (23)$$

where t_r is the conversion from years to growing days and δ_r is resin density. Combining Eqs. 20–23, we can write the relationship between host vigor and the maximum rate of resin production as

$$f_o S_o = \nu L \frac{(1 - m_r)c_r t_r}{(1 - m_w)c_w \delta_r} \quad (24)$$

The dimensionless attack density \tilde{A} and dimensionless parameter γ can be transformed to the empirical scales of Fig. 1 as follows. Let \hat{A} be the number of beetle attacks per unit bark area and ν be host vigor as presented in the data. Using the relationships given by Eqs. 14 and 24, we can relate the model predictions to the empirical data by

$$\hat{A} = \tilde{A} \frac{h_o r_o x}{g_o} \tag{25}$$

$$\nu = \gamma \frac{R_m^2 h_o (1 - m_w) c_w \delta_r}{L (1 - m_r) c_r t_r} \tag{26}$$

The parameter r_o is the maximum resin volume per volume of phloem tissue, which emerges from expressing the maximum resin volume as $R_m = r_o x B$, where x is phloem thickness and B is the tree bark area.

Parameterization

Many of the parameters in Eqs. 25 and 26 are well established in the literature, while others can be estimated within a range. To compare our model predictions with the empirical data shown in Fig. 1, we parameterize our model from studies that are independent of these data (Table 2). The only exception to this are the parameters L and B , which collectively describe the size of an average tree in the study. Because we obtain estimates or ranges for all model parameters, no model fitting is required and the contrast between model prediction and data is a quantitative and independent test of the model. Using the values from Table 2, we can write as $\hat{A} = 427\tilde{A}$, $\nu = 24186\gamma$, and $0.47 \leq \zeta \leq 1.89$, where the range in ζ reflects the estimated range in the sieve tube loss rate k_o . The

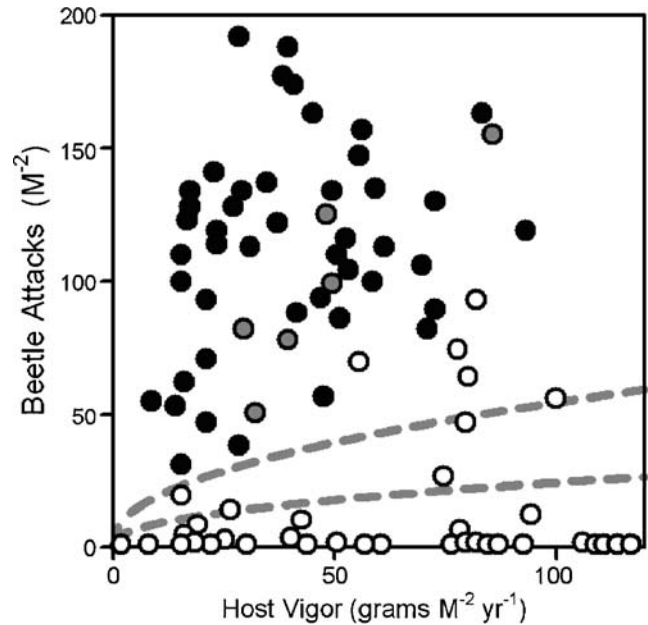


Fig. 7 Predicted threshold for successful attack of Mountain Pine Beetles as a function of host vigor (*dashed lines*). All rate parameters in the model are estimated independently using literature data. The range reflects the uncertainty in the sieve tube loss rate k_o . The *upper line* is $\zeta = 0.47$ and the *lower line* is $\zeta = 1.89$. Empirical data are shown with *circles* as in Fig. 1

predicted threshold from the parameterized linear model is shown in Fig. 7.

Discussion

The work of Berryman et al. (1989), Stenseth (1989), and Powell et al. (1996) provide the first dynamic models of the interaction between bark beetles and host trees that explicitly describes resin defenses. These models also include continuous recruitment of flying beetles to the population of beetles that are attacking

Table 2 Literature parameters for the linear model

Parameter	Description	Value	Source
R_o	Initial resin volume	$0.01 R_m$ (l)	1
r_o	Maximum resin concentration	327 (l m ⁻³)	2
R_m	Maximum resin volume	46.1 (l)	3
h_o	Beetle mortality rate per resin	0.0003869 (l ⁻¹ day ⁻¹)	4
g_o	Resin loss rate per beetle	$4.44e-6$ (A ⁻¹ day ⁻¹)	5
k_o	Sieve tube loss rate per beetle	$2.1e-6 - 8.4e-6$ (A ⁻¹ day ⁻¹)	6
L	Leaf area	20 (m ²)	7
m_w	Wood production cost	0.305 (g g ⁻¹)	8
c_w	Wood mass per carbon mass	1.96 (g g ⁻¹)	9
m_r	Resin production cost	0.69 (g g ⁻¹)	10
c_r	Resin mass per carbon mass	1.14 (g g ⁻¹)	11
t_r	Time conversion to growing days	0.0056 (y day ⁻¹)	12
δ_r	Resin density	854.7 (g l ⁻¹)	13
x	Phloem thickness	0.015 (m)	14

Source details are given in Appendix D

each host. However, data on the threshold for successful attack in natural systems suggest that the dynamics of flying beetles are not involved in the beetle–host interaction, except to establish initial conditions (Christiansen et al. 1987; Mulock and Christiansen 1986, Fig. 1). To understand the core beetle–host interaction in these models, we reanalyzed the models of Berryman et al. (1989), Stenseth (1989), and Powell et al. (1996) in the absence of recruitment from flying beetles. Our results show that the modified models still predict a steady state with live beetles and a dead host, but the steady state is unstable. We therefore conclude that the stability observed in the original models is the result of continuous recruitment from the flying beetle population. While such recruitment is an important process, the beetle–host interaction in natural systems is stable at the scale of an individual tree in the absence of such recruitment, suggesting that the representation of the core beetle–host interaction needs further development.

One process absent from the models of Berryman et al. (1989), Stenseth (1989), and Powell et al. (1996) is an explicit representation of host damage from attacking beetles. The model developed here extends previous models to include host damage. We demonstrated that including explicit host damage produces the same qualitative steady states as previous models (i.e., living beetles with a dead host and dead beetles with a living host) but that both are now stable. Our new model also predicts that the steady states are infinite sets, which implies that the final density of attacking beetles in a dead host, and the final level of host damage, can take on a range of values that depends on the dynamics of the system and the initial abundance of resin and beetles. Biologically, there is good evidence to suggest that this is more realistic than a point steady state (e.g., Christiansen et al. 1987).

The steady states of our new model are in good qualitative agreement with empirical data. However, because all parameters are estimated independently from the literature, the model can be further validated by comparing the predicted threshold for successful beetle attack against data. Our analysis is the first work to quantitatively predict the successful attack threshold for bark beetles based on underlying biological mechanisms. Model predictions are superimposed over the empirical threshold in Fig. 7. The model underestimates the attack threshold over the range of uncertainty in the point estimate of parameter k_o , but the upper predicted threshold is reasonably close to the observed threshold. Given the assumptions that are required to link host vigor to resin production, and the assumption that all trees have the same average characteristics (e.g., bark

area, phloem thickness, and leaf area), the agreement between model prediction and data is encouraging and gives us some faith that the model reflects the biological processes in natural systems.

One key assumption of our model is that aggregation dynamics occur over sufficiently fast time scales that they can be subsumed into the initial conditions of the host–pathogen interaction. To assess the appropriateness of this assumption, we compared our simplified model with one where aggregation dynamics were modeled explicitly (Appendix E). Using aggregation dynamics obtained from an empirical study, the simplified model produces dynamics that are in excellent agreement with the full model (Fig. 9), which provides strong support that our assumption is appropriate. Moreover, this comparison indicates how studies of the bark-beetle system can benefit from separating ecological dynamics into two stages: the first stage considers the aggregation dynamics that map densities of emerging beetles to densities of attacking beetles on host trees, and the second stage considers the fate of the host–pathogen interaction given a set of attack densities.

Host resistance to bark beetles is described by the attack threshold. In our model, the threshold is determined by the parameters γ and ζ . The parameter γ is the maximum rate of resin production per resin volume divided by the maximum beetle mortality rate. Thus, hosts with greater ability to produce resin on a per capita scale are more resistant to beetle attacks. The model also suggests that host vigor may be refined further if it is calculated relative to the susceptibility of different beetle species to resin defenses. The second parameter ζ is the ratio of the sieve tube damage rate divided by the resin loss rate. Beetles that damage host trees faster reduce the threshold required to kill a host. Thus, the model suggests that beetle success is improved by increasing how quickly they can damage the host tissue and tolerate resin rather than by the ability to remove resin.

As a result of the economic impact of bark beetles, there is a wealth of empirical data that can be used to validate models of the host–pathogen interaction. The agreement between model prediction and the empirical threshold found here suggests that our new model captures aspects of the natural host–pathogen interaction that occur between aggregation events. However, a more rigorous test of any model is the ability to predict not only the final state abundances but also the time required to reach steady state. Empirical observations of successfully attacked host trees suggest that attacking beetles can colonize the entire bark area of a host over a time span of four to six weeks (e.g., Kirisits and Offenthaler 2002). Using the estimated parameters,

the model predicts that the time for half of the bark area to be damaged is over 200 days, which is much longer than the colonization time observed in natural systems. Thus, while the model developed here captures the threshold for attack, there still remains scope for further development. Our present analysis focuses on model predictions using only point estimates of the parameters. As new empirical data become available for this system, more robust point estimates can be developed and the analysis can be expanded to incorporate the variance and covariance in parameter estimates. Furthermore, by developing resin production functions (Eq. 24) that include more detailed physiological processes, the model presented here can be expanded to consider situations where tree growth is limited by both carbohydrates and nutrients.

The general model developed here describes the fate of the beetle–host interaction through the processes of resinous defenses and host damage. For a wide class of functions, the model predicts that the steady states are infinite sets, which is more consistent with empirical observations than previous models. The linear version of the model does reasonably well at predicting the empirical threshold when parameterized to independent data. However, there is clearly room for improvement. In particular, we feel that a better understanding of the functions and parameters that describe the biological processes will be invaluable towards assessing the utility of the model proposed here. The advantage of establishing a single framework to investigate beetle–host systems is to compare across species that have markedly different success in attacking host trees. For example, are some species less successful because they have less tendency to aggregate, or because they are less able to damage a host? Because beetle survival is determined to a large extent by the ability to kill a host tree, the threshold for successful attack generates a strong Allee effect in bark beetles at the population scale. Thus, understanding how the characteristics of each beetle species determine the successful attack threshold will help us understand and predict the population dynamics of different bark beetle species.

Acknowledgements We would like to thank Alex Potapov and Frank Hilker for independently solving the phase-plane trajectories used in Appendix B, and two anonymous reviewers who helped improve the manuscript. This study was funded by Natural Resources Canada–Canadian Forest Service under the Mountain Pine Beetle Initiative. Publication does not necessarily signify that the contents of this report reflect the views or policies of Natural Resources Canada–Canadian Forest Service. Additional support was provided by Natural Sciences and Engineering Research Council (NSERC) and Alberta Ingenuity Postdoctoral fellowships to WAN and NSERC Discovery grants and Canada Research Chairs to MAL.

Appendix A

In the absence of recruitment, the beetle–host model presented by Stenseth (1989) is

$$\frac{dA}{dt} = -b_1 AR \quad (27)$$

$$\frac{dR}{dt} = b_2 - b_3 A - (b_4 - b_5 A) R \quad (28)$$

where $A(t)$ is the density of attacking beetles per tree and $R(t)$ is the volume of resin per beetle gallery. Introducing the following dimensionless variables

$$\tilde{A} = A \frac{b_5}{b_4}, \quad \tilde{R} = R \frac{b_5}{b_3}, \quad \tilde{t} = tb_4$$

and the dimensionless parameters

$$\alpha = \frac{b_1 b_3}{b_4 b_5}, \quad \beta = \frac{b_5 b_2}{b_4 b_3}$$

we can write the dimensionless version of the modified model as (after dropping the tildes)

$$\frac{dA}{dt} = -\alpha AR \quad (29)$$

$$\frac{dR}{dt} = \beta - A - R + AR \quad (30)$$

The model given by Eqs. 29 and 30 has two steady states. The first is $(A^*, R^*) = (0, \beta)$, which is a steady state where the tree is alive and all attacking beetles are dead. The second is $(A^*, R^*) = (\beta, 0)$, which is a steady state where the beetles have successfully killed the host tree. The Jacobian of Eqs. 29 and 30 is given by

$$\mathbf{J}_{(A^*, R^*)} = \begin{pmatrix} -\alpha R^* & -\alpha A^* \\ R^* - 1 & A^* - 1 \end{pmatrix} \quad (31)$$

At the steady state $(A^*, R^*) = (0, \beta)$, both eigenvalues are negative, which means that the tree alive steady state is stable. At the steady state $(A^*, R^*) = (\beta, 0)$, one eigenvalue is negative and one is positive. Thus, the tree dead steady state is an unstable saddle.

Appendix B

Stability analysis of the Powell et al. (1996) model in the absence of beetle recruitment (Eqs. 9 and 10). The Jacobian is given by

$$\mathbf{J}_{(H^*, R^*)} = \begin{pmatrix} -R^* & -H^* \\ -R^* & \beta - 2\beta R^* - H^* \end{pmatrix} \quad (32)$$

At the steady state $(H^*, R^*) = (0, 1)$, both eigenvalues are negative and the live host steady state is stable. At

the steady state $(H^*, R^*) = (\bar{H}, 0)$, one of the eigenvalues is zero, which means that the eigenvalues are insufficient for characterizing stability. To investigate stability at this steady state, we study the nonlinear perturbation equations. Let $H(t) = H^* + h(t)$ and $R(t) = R^* + r(t)$, where $h(t)$ and $r(t)$ are small perturbations around the steady state $(H^*, R^*) = (\bar{H}, 0)$ are

$$\frac{dh}{dt} = -r(\bar{H} + h) \tag{33}$$

$$\frac{dr}{dt} = r(\beta - \bar{H} - h) - \beta r^2 \tag{34}$$

We begin by considering the relationship between r and h at the $dr/dh = 0$ isocline (denoted by \hat{r} and \hat{h}).

$$\hat{r} = 1 - \frac{\bar{H} + \hat{h}}{\beta} \tag{35}$$

Because $r \geq 0$ and $dh/dt \leq 0$, the phase-plane trajectories always decrease along h . For values of h greater than the isocline, dr/dt is negative, and for values of h less than the isocline, the gradient dr/dt is positive. This can be seen by substituting the point $h = \hat{h} + \epsilon$ into Eq. 34, which yields

$$\frac{dr}{dt} = -r\epsilon \tag{36}$$

If ϵ is negative, then r will increase, and if ϵ is positive, then r will decrease. The isocline given by Eq. 35 crosses the stable steady state of $\hat{r} = 0$ at the point $(\hat{h}, \hat{r}) = (\beta - \bar{H}, 0)$. The critical trajectory can now be defined as the one that passes through the point $(\hat{h}, \hat{r}) = (\beta - \bar{H}, 0)$ because only trajectories with smaller r (or larger h) than this critical trajectory will be in the basin of attraction of $r^* = 0$. The critical trajectory for the system given by Eqs. 9 and 10 can be solved analytically, which allows us to write the perturbation conditions exactly. By defining $\eta = \ln(\bar{H} + h)$ and $\mu = r \exp(-\beta\eta)$, we can rewrite Eqs. 33–34 as

$$\frac{d\mu}{d\eta} = e^{\eta(1-\beta)} - \beta e^{-\beta\eta} \tag{37}$$

If $\beta \neq 1$, then the solution of Eq. 37 through the critical point $(\hat{h}, \hat{r}) = (\beta - \bar{H}, 0)$ is

$$\hat{r} = \frac{1}{1 - \beta} \left(1 - \beta + \bar{H} + \hat{h} - \left(\frac{\bar{H} + \hat{h}}{\beta} \right)^\beta \right) \tag{38}$$

If $\beta = 1$, then the solution is

$$\hat{r} = 1 + (\bar{H} + \hat{h}) (\ln(\bar{H} + \hat{h}) - 1) \tag{39}$$

The stability criterion for \bar{H} at the steady state $(H^*, R^*) = (\bar{H}, 0)$ can be determined numerically for arbitrary perturbations using Eqs. 38 and 39. As $r \rightarrow 0$ and $h \rightarrow 0$, the stability criterion is $\bar{H} = \beta$.

Appendix C

Stability analysis of the linear host–pathogen model given by Eqs. 16–18. The Jacobian is

$$\mathbf{J}_{(A^*, S^*, R^*)} = \begin{pmatrix} -R^* & 0 & 0 \\ -\zeta S^* & -\zeta A^* & 0 \\ -R^* & \gamma(1 - R^*) & -\gamma S^* - A^* \end{pmatrix} \tag{40}$$

At each of the three steady states $(A^*, S^*, R^*) = (\bar{A}, 0, 0)$, $(0, 0, \bar{R})$, $(0, \bar{S}, 1)$, there is at least one zero eigenvalue, which means that a linear analysis around the steady state is not sufficient to assess stability. To determine stability of the steady states, we study the nonlinear perturbations through simulation. The full perturbation equations for all steady states are

$$\frac{da}{dt} = -(A^* + a)(R^* + r) \tag{41}$$

$$\frac{ds}{dt} = -\zeta(A^* + a)(S^* + s) \tag{42}$$

$$\frac{dr}{dt} = \gamma(S^* + s)(1 - R^* - r) - (A^* + a)(R^* + r) \tag{43}$$

where $a = A - A^*$, $s = S - S^*$, and $r = R - R^*$ are perturbations around the steady state (A^*, S^*, R^*) . The perturbations surrounding each steady state are obtained by setting $(A^*, S^*, R^*) = (\bar{A}, 0, 0)$, $(0, 0, \bar{R})$, or $(0, \bar{S}, 1)$. Because a and s can only decrease, stability for all steady states is assessed by whether or not r decays to zero. Unless otherwise noted, we explored the parameter space of ζ and γ from zero to 10^{10} (i.e., $0 \leq \zeta \leq 10^{10}$ and $0 \leq \gamma \leq 10^{10}$).

Near the steady state $(A^*, S^*, R^*) = (0, \bar{S}, 1)$, r decays to zero from the initial conditions of $(a_o, s_o, r_o) = (10^{-8}, 10^{-8}, -10^{-8})$ for all values of ζ explored, all values of $0 \leq \bar{S} \leq 1$, and for values of $\gamma > 0$. Thus, we conclude that the steady state $(A^*, S^*, R^*) = (0, \bar{S}, 1)$ is stable.

Near the steady state $(A^*, S^*, R^*) = (0, 0, \bar{R})$, r increases to $r^* = 1 - \bar{R}$ from the initial conditions of $(a_o, s_o, r_o) = (10^{-8}, 10^{-8}, 0)$ for all values of ζ explored, all values of $0.01 \leq \bar{R} \leq 1$, and for values of $\gamma > 0$. Values of $\bar{R} < 0.01$ yielded unreliable numerical simulations for small values of γ . Thus, for $\gamma > 0$ and $\bar{R} \geq 0.01$, the steady state $(A^*, S^*, R^*) = (0, 0, \bar{R})$ is unstable.

The steady state $(A^*, S^*, R^*) = (\bar{A}, 0, 0)$ is a little different from the others in that it is locally stable but

not globally stable for \bar{A} bounded away from zero. For a given set of parameters, a sufficiently small perturbation could be found such that r decayed to zero. Specifically, $(a_o, r_o, s_o) = (0, \epsilon, \epsilon)$, r decays to zero for ϵ sufficiently small, for $10^{-10} \leq \zeta \leq 10^{10}$, $0 \leq \gamma \leq 10^{10}$, and $\bar{A} \geq 0.01$. We did not check $0 < \zeta < 10^{-10}$, and values of $\bar{A} < 0.01$ yielded unreliable numerical simulations. Thus, for slightly positive values of ζ and $\bar{A} \geq 0.01$, the steady state $(A^*, S^*, R^*) = (\bar{A}, 0, 0)$ is stable.

Appendix D

1. Initial resin density, relative to R_m , is always low (e.g., Raffa and Smalley 1995). We assume $R_o = 0.01 R_m$ based on Wallin and Raffa (1999).
2. Raffa and Smalley (1995) report a maximum monoterpene concentration of 305 mg per gram of dried phloem. Assuming a resin density of 0.858 g ml⁻¹ based on the largest component of resin α -pinene, a dried phloem density of 0.46 g cm⁻³ (Bouffier et al. 2003), and a monoterpene concentration in resin of 0.5, we estimate a maximum resin concentration of $r_o = 327$ (l m⁻³).
3. Maximum resin volume can be estimated from $R_m = r_o x B$, where x is phloem thickness and B is bark area. From Waring and Pitman (1985), the average bark area was $B = 9.4$ (m²). Assuming an average phloem thickness of $x = 0.015$ (m) (e.g. Zausen et al. 2005) gives an estimate of $R_m = 46.1$ (l).
4. Raffa and Berryman (1983) report a 30% beetle mortality rate over a ~20-day period in host trees that are killed by mountain pine beetles. If we assume that resin volume was maximal (i.e., R_m), then this gives a rough mortality rate estimate of $h_o = 0.0003869$ (l⁻¹ day⁻¹).
5. From Raffa and Smalley (1995), we can get an estimate for the resin loss rate within the fungal/beetle activity zone (g_z). Using an initial resin concentration of 250 mg per gram, and a final concentration of 210 mg per gram over a 15-day period, we estimate the loss rate of resin within the fungal zone as $g_z = 0.0116$ (A⁻¹ day⁻¹). To convert this into a per-capita loss rate of resin over the entire tree from each attack, we use the sampled lesion size of 36 cm² from Raffa and Smalley (1995), and the average bark area of $B = 9.4$ (m²) from Waring and Pitman (1985), to estimate a resin loss rate of $g_o = 4.4 \times 10^{-6}$ (A⁻¹ day⁻¹).
6. The linear growth of the damaged area is roughly between 0.5 and 1 cm per day (Reid et al. 1967). Thus, we assume an area increment in the range of

0.196–0.785 cm² per day of damaged tissue. If we assume that sieve tube damage is best accounted for by the area of damage per area of bark, then, assuming an average bark area of $B = 9.4$ (m²) from Waring and Pitman (1985), the sieve tube damage rate is given by the range of $k_o = 2.1 \times 10^{-6}$ to $k_o = 8.4 \times 10^{-6}$.

7. Using the average DBH of 0.15 (m) from Waring and Pitman (1985), the sapwood area to DBH relationship from Bond-Lamberty et al. (2002), and the sapwood area to leaf area relationship from Callaway et al. (1994) for lodgepole pines, we estimate the average leaf area for the site as $L = 20$ (m²).
8. From Lavigne and Ryan (1997). Value used is averaged over locations and age classes and agrees well with the estimate for generic wood of $m_w = 0.25$ (Penning de Vries 1975).
9. Czimezik et al. (2002).
10. From Gershenson (1994), the metabolic cost of producing monoterpenes is 3.54 (g g⁻¹) of glucose per monoterpene. Using the molar mass of monoterpenes (136.23 g Mol⁻¹) and glucose (180.16 g Mol⁻¹), the total carbon cost by mass is 3.2 g glucose per gram of resin. Converting this to a dimensionless proportion yields $m_r = 0.69$ (g g⁻¹).
11. From the molar mass of monoterpenes (136.23 g Mol⁻¹), $c_r = 1.14$ (g g⁻¹).
12. Assuming a 180-day growing season.
13. Using a resin density of 0.858 g ml⁻¹ for pinene, which is the most abundant component of resin.
14. We assume a typical value of $x = 0.015$ (m) (e.g., Zausen et al. 2005).

Appendix E

The model given by Eqs. 16–18 assumes that the time-scale of beetle aggregation to a host tree is sufficiently fast, relative to the time-scale of the attack dynamics, that the process of aggregation can be subsumed into the initial conditions of the model (i.e., A_o). To assess the validity of this assumption, we can explicitly incorporate aggregation dynamics and compare this with the simplified model. The dimensional model with aggregation dynamics is given by

$$\frac{dA}{dt} = A_o \Gamma(t, \alpha, \beta) - h_o A R \quad (44)$$

$$\frac{dS}{dt} = -k_o A S \quad (45)$$

$$\frac{dR}{dt} = f_o \left(1 - \frac{R}{R_m}\right) S - g_o A R \quad (46)$$

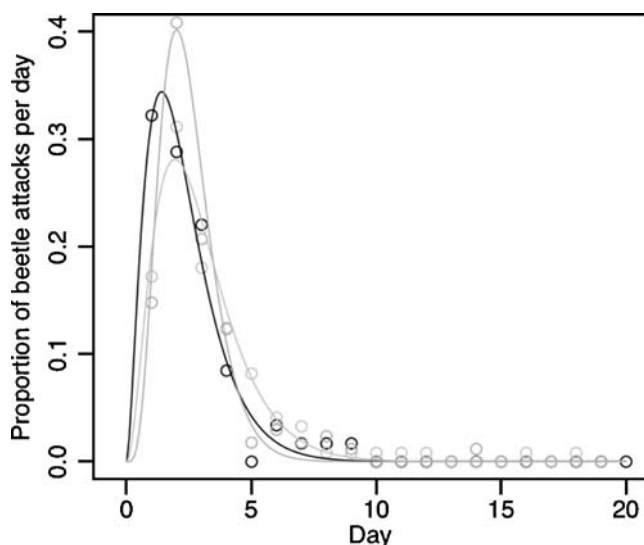


Fig. 8 Proportion of beetle attacks through time from Raffa and Berryman (1983). Circles are digitized data and lines are fit gamma distribution. Black shows dynamics in 1977, dark gray those in 1978, and light gray those in 1979

where $\Gamma(t, \alpha, \beta)$ describes the proportion of the total attacking beetles (A_o) that arrive at time t . To parameterize the aggregation distribution for an empirical ex-

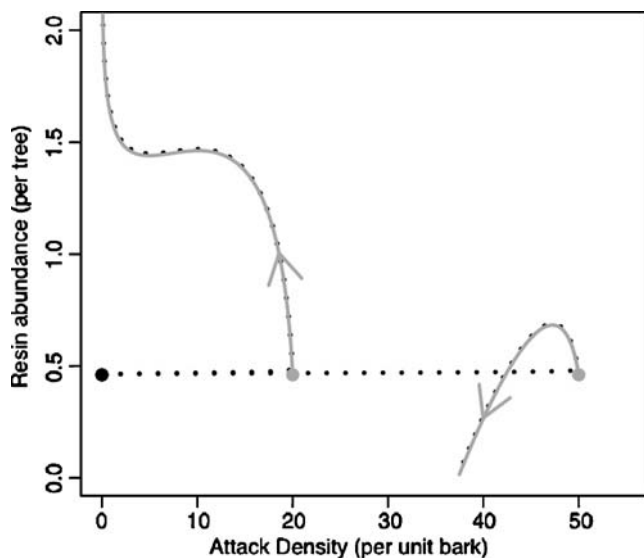


Fig. 9 Dynamics of the attack process for two levels of attack density ($A_o = 20$ and $A_o = 50$). Black dots show dynamics when aggregation is explicitly incorporated Eqs. 44–46, and gray lines show dynamics under the simplifying assumption that aggregation can be subsumed into an initial attack density A_o Eqs. 16–18. Circles denote initial conditions for both models, and arrows show the direction of time. Note that the gray lines overlay the black dots for much of the dynamics. Despite the differing initial conditions, time trajectories of the simplified model approach that of the full model with explicit aggregation, which suggests that the simplified model is a good approximation to the asymptotic dynamics of the full model well. All other parameter values are given in Table 2

ample, we fit the distribution to the arrival data in Fig. 1 of Raffa and Berryman (1983). Fitting the function yields parameter estimates of $\alpha = \{2.61, 5.21, 3.01\}$ and $\beta = \{0.87, 0.47, 0.96\}$ for the years 1977, 1978, and 1979 (Fig. 8). To demonstrate the impact of incorporating both time-scales, we use the mean parameter estimates of $\alpha = 3.61$ and $\beta = 0.77$. Figure 9 shows predicted dynamics of the attack process under both models. The similarity of the dynamics demonstrates that the simplifying assumption of subsuming the aggregation process into an initial condition is a good approximation to the full model.

References

- Allee W (1931) Animal aggregations. The University of Chicago Press, Chicago
- Berryman A (1979) Dynamics of bark beetle populations: analysis of dispersal and redistribution. Bull Soc Entomol Suisse 52:227–234
- Berryman A, Stenseth N (1989) A theoretical basis for understanding and managing biological populations with particular reference to the spruce bark beetle. Holarct Ecol 12:387–394
- Berryman A, Raffa K, Millstein J, Stenseth N (1989) Interaction dynamics of bark beetle aggregation and conifer defense rates. OIKOS 56:256–263
- Bond-Lamberty B, Wang W, Gower S (2002) Aboveground and belowground biomass and sapwood area allometric equations for six boreal tree species of northern alberta. Can J For Res 32:1441–1450
- Bouffier L, Gartner B, Domec J (2003) Wood density and hydraulic properties of ponderosa pine from the willamette valley vs. the cascade mountains. Wood Fiber Sci 35(2):217–233
- Callaway R, DeLucia E, Schlesinger W (1994) Biomass allocation of montane and desert ponderosa pine: an analog for response to climate change. Ecology 75(5):1474–1481
- Christiansen E, Waring R, Berryman A (1987) Resistance of conifers to bark beetle attack: searching for general relationships. For Ecol Manag 22:89–106
- Courchamp F, Clutton-Brock T, Grenfell B (1999) Inverse density dependence and the allee effect. Trends Ecol Evol 14(10):405–410
- Czimezik C, Preston C, Schmidt M, Werner R, Schulze E (2002) Effects of charring on mass, organic carbon, and stable carbon isotope composition of wood. Org Geochem 33: 1207–1223
- Franceschi V, Krokene P, Christiansen E, Krekling T (2005) Anatomical and chemical defenses of conifer bark against bark beetles and other pests. New Phytol 167:353–376
- Gershenson J (1994) Metabolic cost of terpenoid accumulation in higher plants. J Chem Ecol 20(6):1281–1328
- Kirisits T, Offenthaler I (2002) Xylem sap flow of norway spruce after inoculation with the blue stain fungus *Ceratocystis polonica*. Plant Pathol 51:359–364
- Lavigne M, Ryan M (1997) Growth and maintenance respiration rates of aspen, black spruce and jack pine stems at northern and southern boreas sites. Tree Physiol 17:543–551
- Lewinsohn E, Gijzen M, Croteau R (1991) Defence mechanisms of conifers. Plant Physiol 96:44–49

- Logan J, Powell J (2001) Ghost forests, global warming, and the mountain pine beetle. *Am Entomol* 47:160–173
- Lombardero ML, Ayres MP, Lorio PL Jr, Ruel JJ (2000) Environmental effects on constitutive and inducible defences of *Pinus taeda*. *Ecol Lett* 3:329–339
- Loomis W (1932) Growth-differentiation balance vs. carbohydrate-nitrogen ratio. *Proc Am Soc Hortic Sci* 29: 240–245
- Miller R, Berryman A (1986) Carbohydrate allocation and mountain pine beetle attack in girdled lodgepole pines. *Can J For Res* 16(5):1036–1040
- Mulock P, Christiansen E (1986) The threshold of successful attack by *Ips typographus* on *Picea abies*: a field experiment. *For Ecol Manag* 14:125–132
- Ogden N, Casey A, French N, Adams J, Woldehiwet Z (2002) Field evidence for density-dependent facilitation amongst *Ixodes ricinus* ticks feeding on sheep. *Parasitology* 124:117–125
- Penning de Vries F (1975) Use of assimilates in higher plants. In: Cooper JP (ed) *Photosynthesis and productivity in different environments*. Cambridge University Press, Cambridge, pp 459–480
- Powell J, Logan J, Bentz B (1996) Local projections for a global model of mountain pine beetle attacks. *J Theor Biol* 179(3):243–260
- Raffa K (2001) Mixed messages across multiple trophic levels: the ecology of bark beetle chemical communication systems. *Chemoecology* 11:49–65
- Raffa K, Berryman A (1983) The role of host plant resistance in the colonization behavior and ecology of bark beetles (coleoptera:scolytidae). *Ecol Monogr* 53(1):27–49
- Raffa K, Smalley E (1995) Interaction of pre-attack and induced monoterpene concentrations in host conifer defense against bark beetle-fungal complexes. *Oecologia* 102: 285–295
- Raffa K, Aukema B, Erbilgin N, Klepzig K, Wallin K (2005) Interactions among conifer terpenoids and bark beetles across multiple levels of scale: an attempt to understand links between population patterns and physiological processes. *Recent Adv Phytochem* 39:79–118
- Reid R, Whitney H, Watson J (1967) Reactions of lodgepole pine to attack by *Dendroctonus ponderosae* hopkins and blue stain fungi. *Can J Bot* 45:1115–1126
- Stenseth N (1989) A model for the conquest of a tree by bark beetles. *Holarct Ecol* 12:408–414
- Thompson M, Holbrook N (2003) Scaling phloem transport: water potential equilibrium and osmoregulatory flow. *Plant Cell Environ* 26:1561–1577
- Trapp S, Croteau R (2001) Defensive resin biosynthesis in conifers. *Annu Rev Plant Physiol Plant Mol Biol* 52:689–724
- Turtola A, Manninen A, Rikala R, Kainulainen P (2003) Drought stress alters the concentration of wood terpenoids in scots pine and norway spruce seedlings. *J Chem Ecol* 29(9): 1981–1995
- Uma Devi K, Uma Maheswara Rao C (2006) Allee effect in the infection dynamics of the entomopathogenic fungus *Beauveria bassiana* (bals) vuill. on the beetle, *Mylabris pustulata*. *Mycopathologia* 161:385–394
- Vanninen P, Mäkelä A (2005) Carbon budget for scots pine trees: effect of size, competition and site fertility on growth allocation and production. *Tree Physiol* 25:17–30
- Wallin K, Raffa K (1999) Altered constitutive and inducible phloem monoterpenes following natural defoliation of jack pine: implications to host mediated interguild interactions and plant defense theories. *J Chem Ecol* 25(4):861–880
- Wallin K, Raffa K (2001) Effects of folivory on subcortical plant defenses: can defense theories predict interguild processes? *Ecology* 82(5):1387–1400
- Waring R, Pitman G (1985) Modifying lodgepole pine stands to change susceptibility to mountain pine beetle attack. *Ecology* 66(3):889–897
- Waring R, Thies W, Muscato D (1980) Stem growth per unit of leaf area: a measure of tree vigor. *For Sci* 1:112–117
- Zausen G, Kolb T, Bailey J, Wagner M (2005) Long-term impacts of stand management on ponderosa pine physiology and bark beetle abundance in northern arizona: a replicated landscape study. *For Ecol Manag* 218:291–305
- Zhang Y, Reed D, Cattellino P, Gale M, Jones E, Liechty H, Mroz G (1994) A process-based growth model for young red pine. *For Ecol Manag* 69:21–40